

Supplemental Information

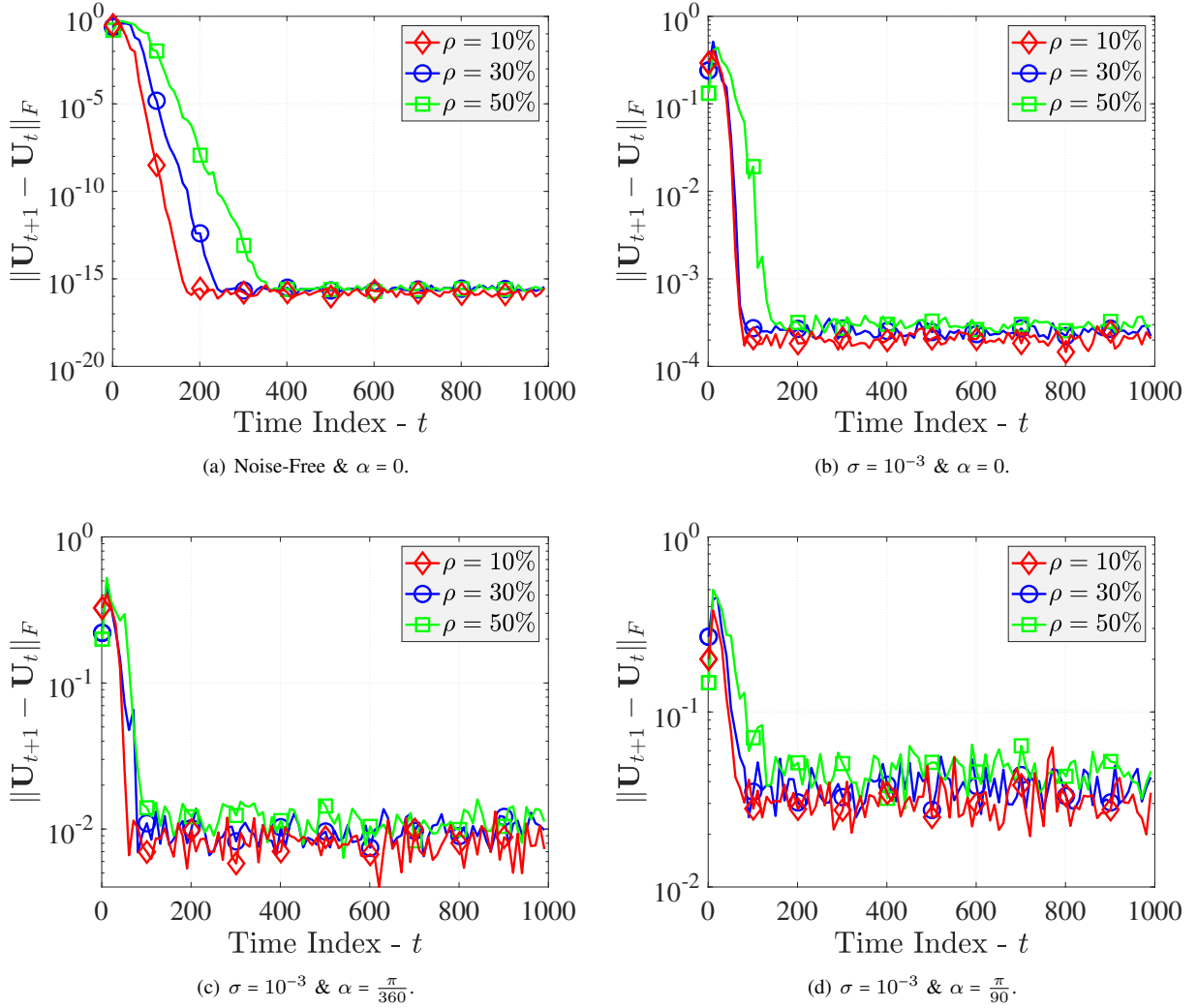


Fig. S1 – Convergence of ACP in terms of the variation $\| \mathbf{U}_{t+1} - \mathbf{U}_t \|_F$: On a synthetic tensor whose size is $20 \times 20 \times 20 \times 1000$ and its CP rank 5.

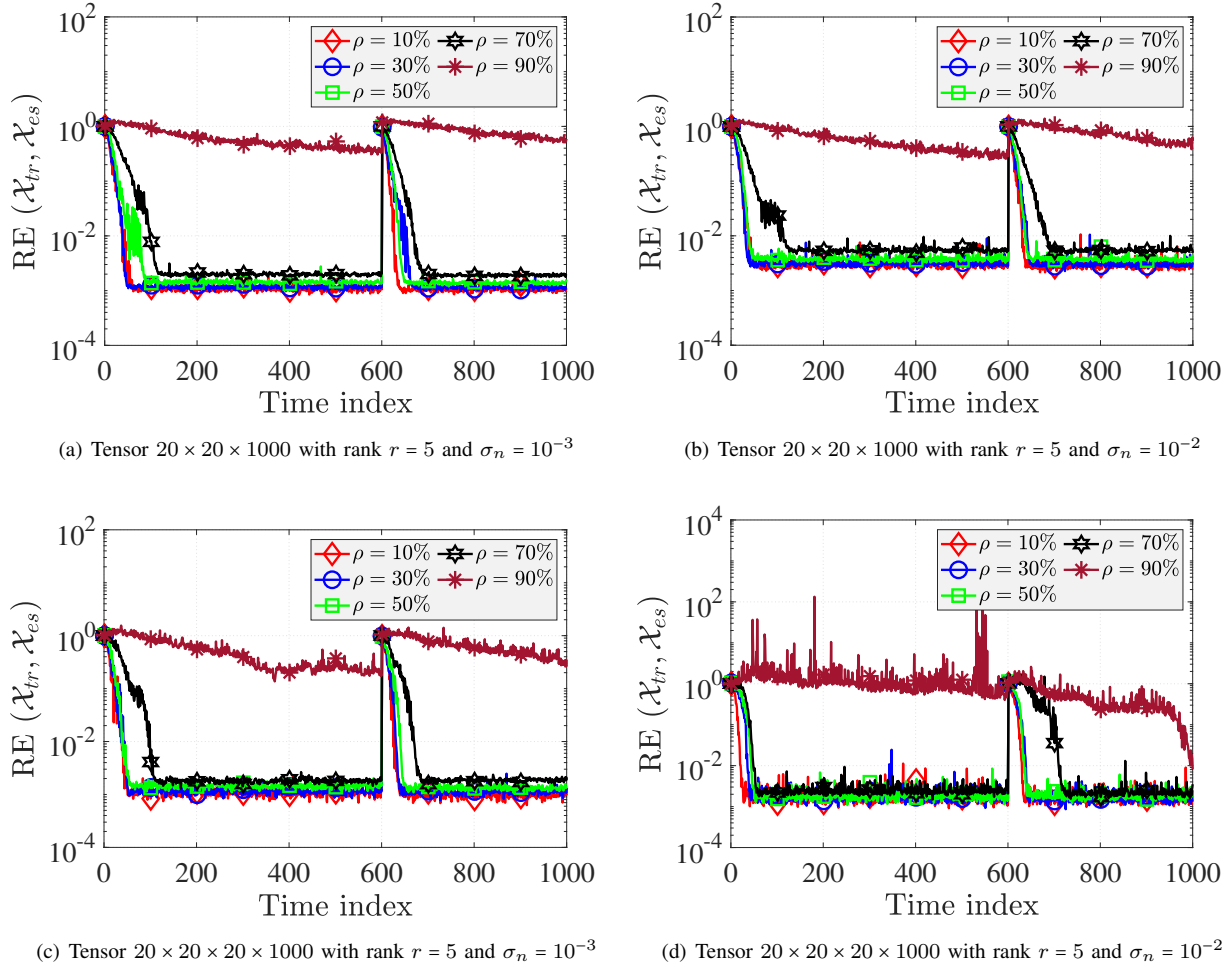


Fig. S2 – Effect of missing data on the performance of ACP with different levels of missing density from 10% to 90%.

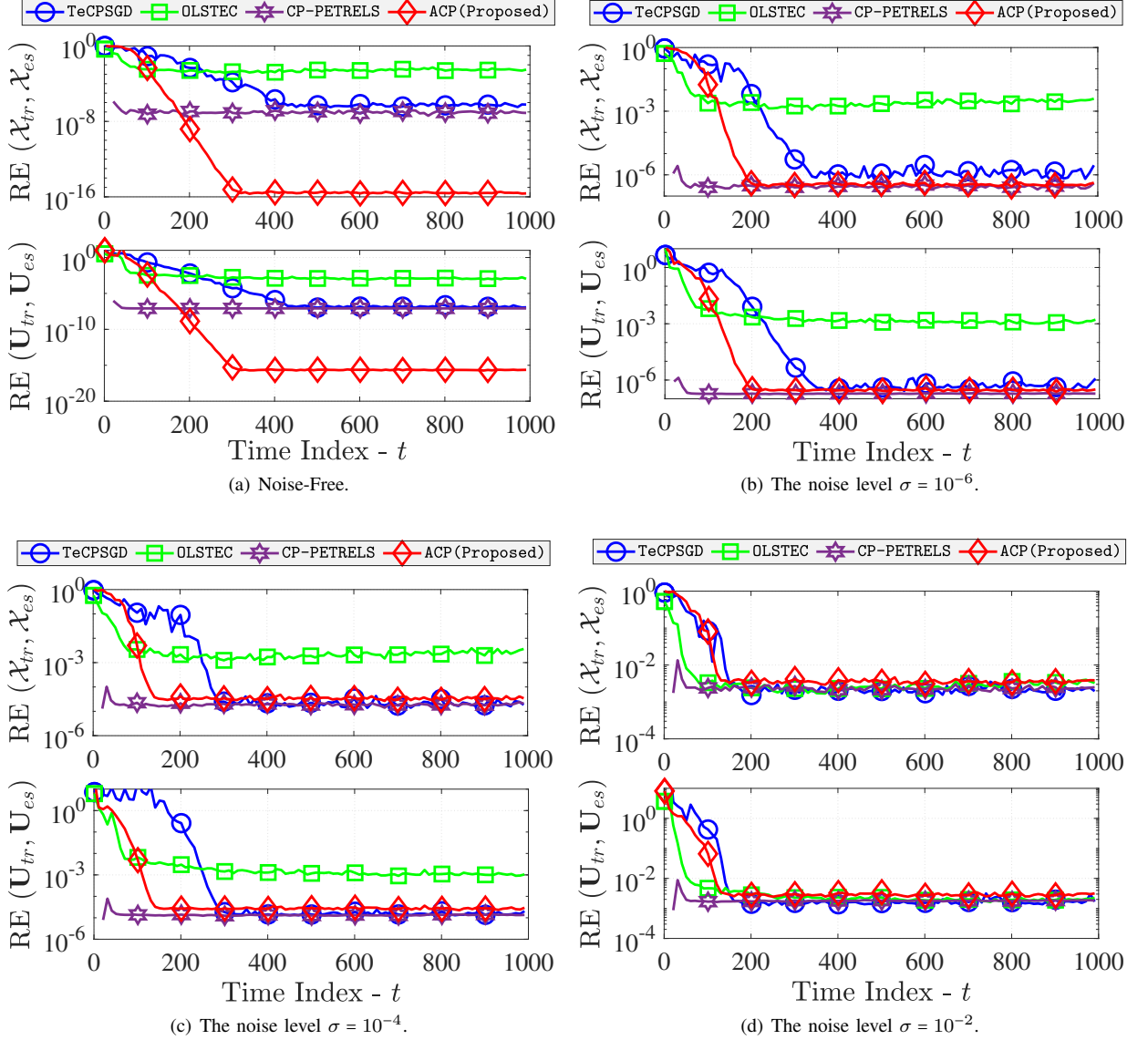


Fig. S3 – Performance of adaptive CP decompositions versus the noise level: On a static tensor whose size is $20 \times 20 \times 20 \times 1000$ and its CP rank 5; 50% observations are missing.

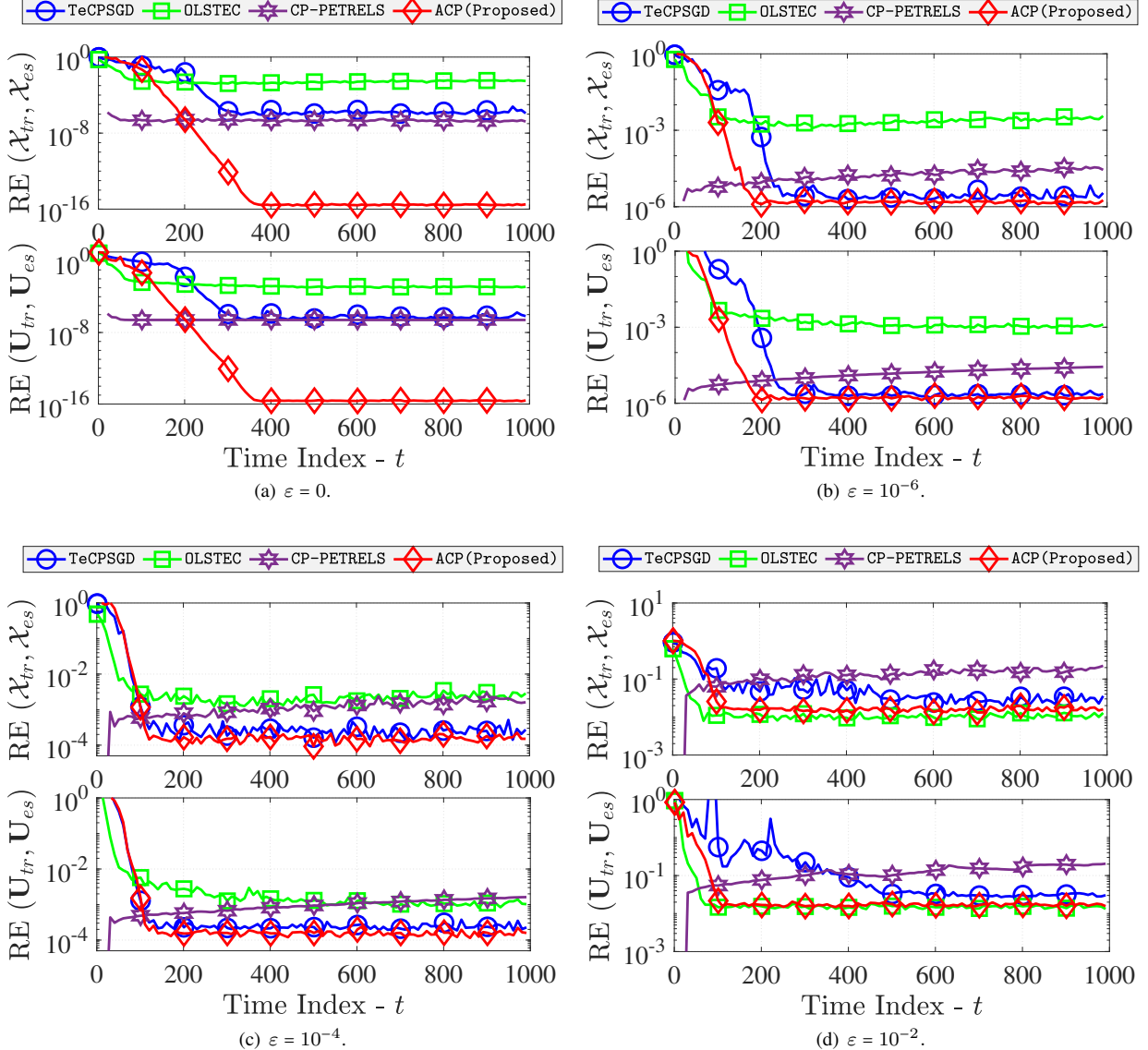


Fig. S4 – Performance of adaptive CP decompositions versus the time-varying factor ε : On a free-noise tensor whose size is $20 \times 20 \times 20 \times 1000$ and its CP rank 5; 90% observations are missing.

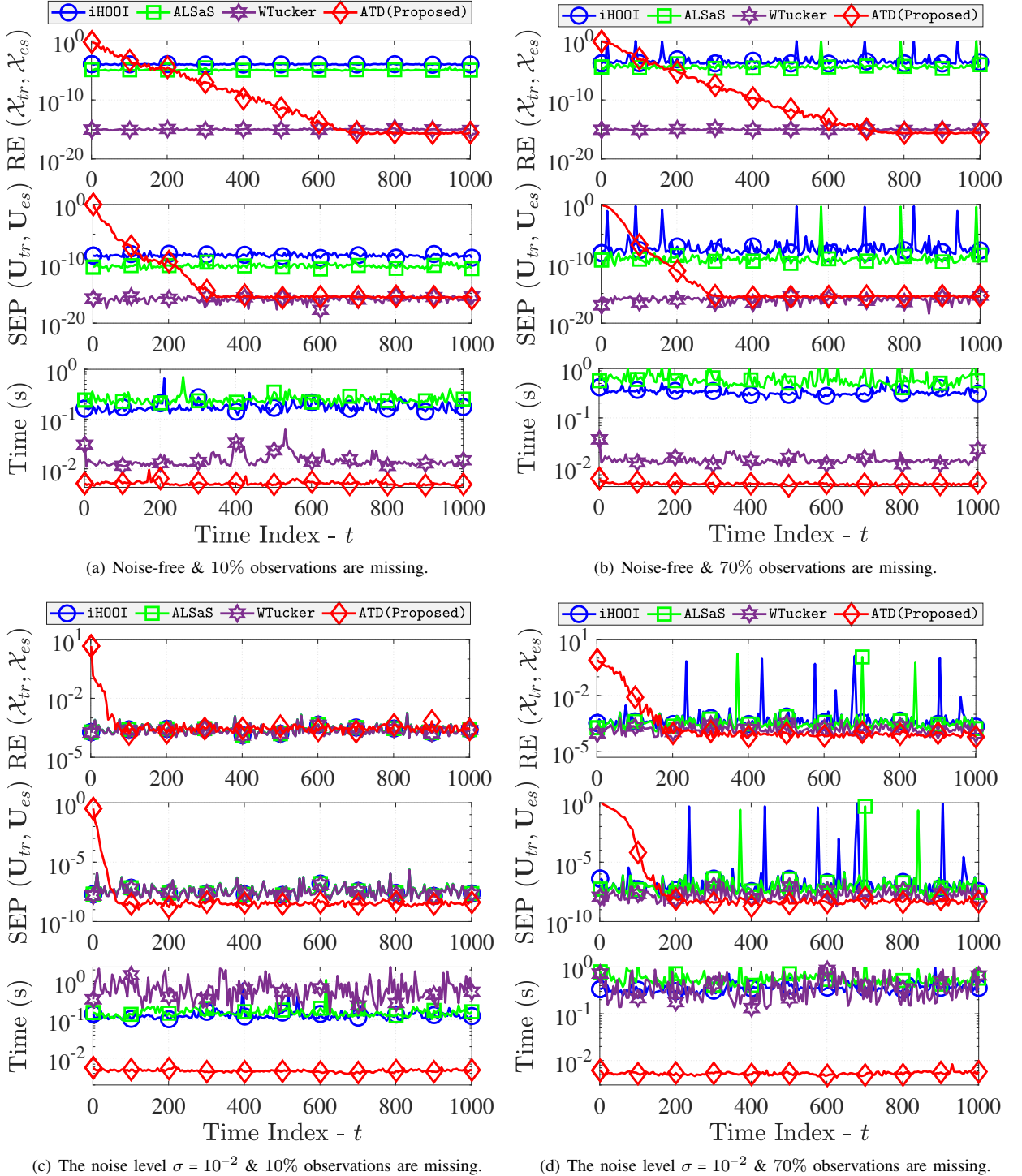


Fig. S5 – Performance of Tucker decompositions for tensor completion: On a synthetic tensor whose size is $20 \times 20 \times 20 \times 1000$ and its Tucker rank $[3, 3, 3, 3]$.

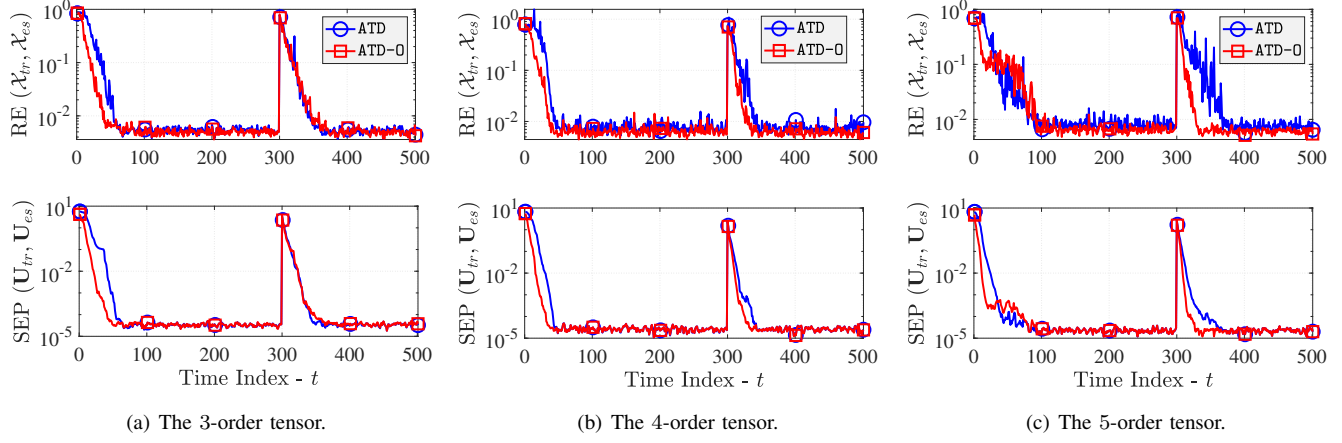


Fig. S6 – Performance comparison between the unconstrained ATD and orthogonal ATD: 30% observations are missing, the noise level $\sigma = 10^{-3}$ and the time-varying factor $\varepsilon = 10^{-3}$.

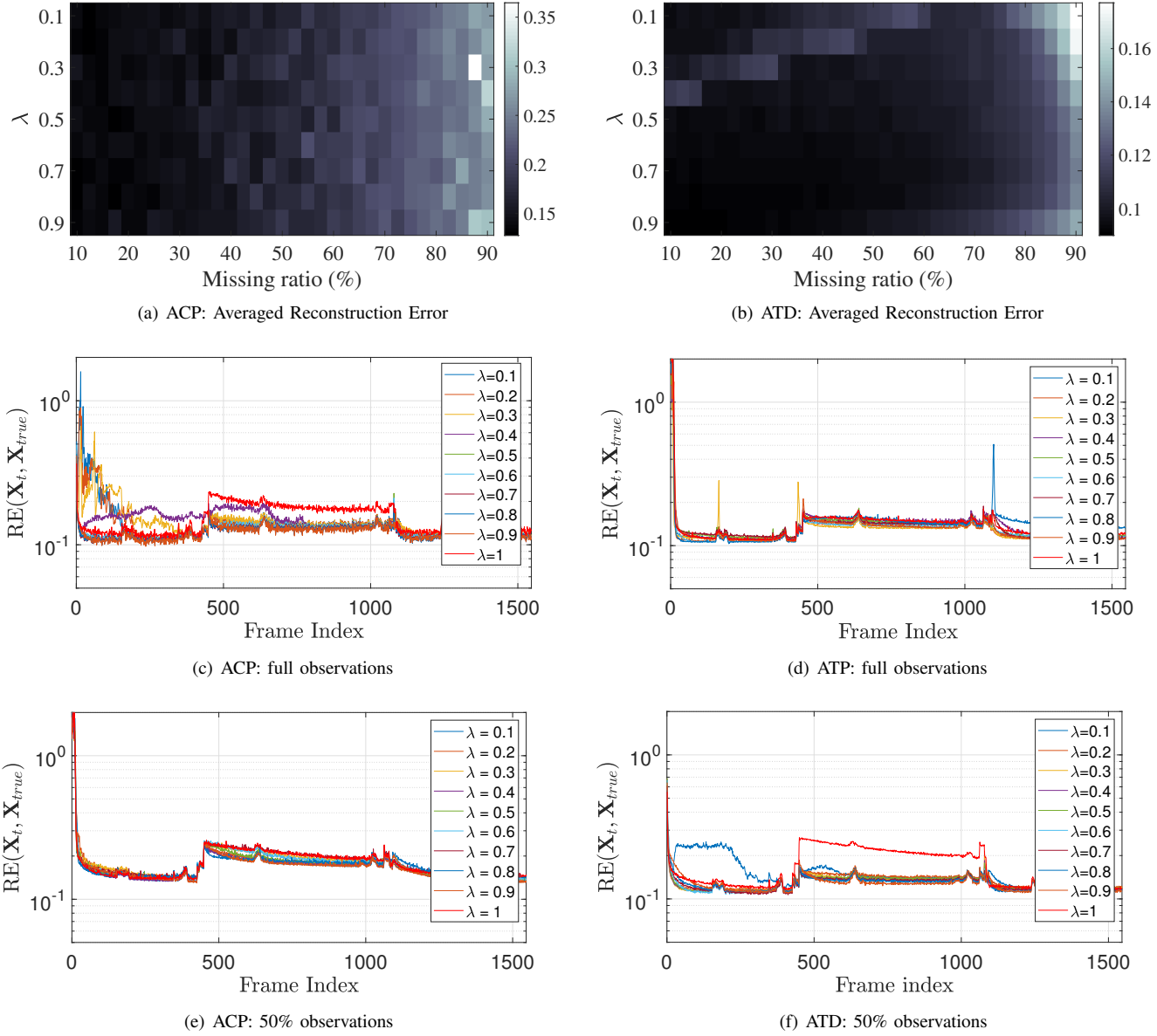


Fig. S7 – Effect of the forgetting factor λ on the video completion accuracy of ACP and ATD on Lobby data.

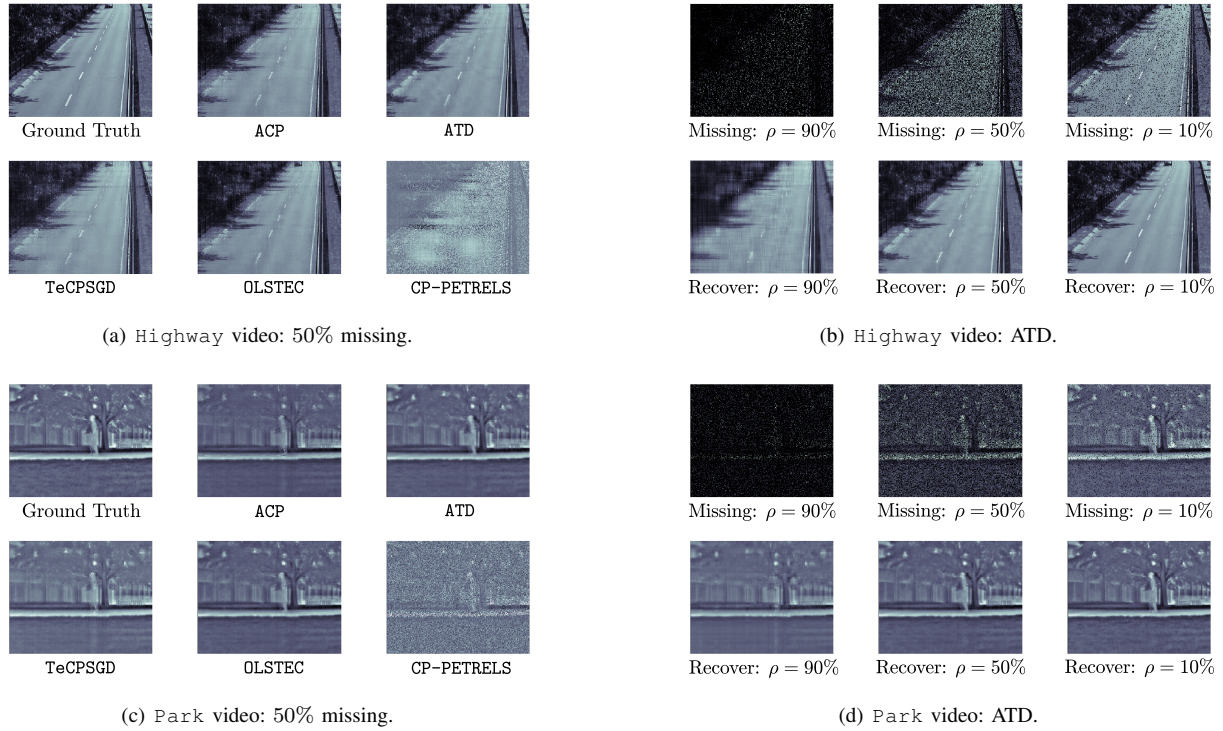


Fig. S8 – Performance of adaptive tensor decompositions on surveillance video sequences.



Fig. S9 – Performance of adaptive tensor decompositions on Lobby data.

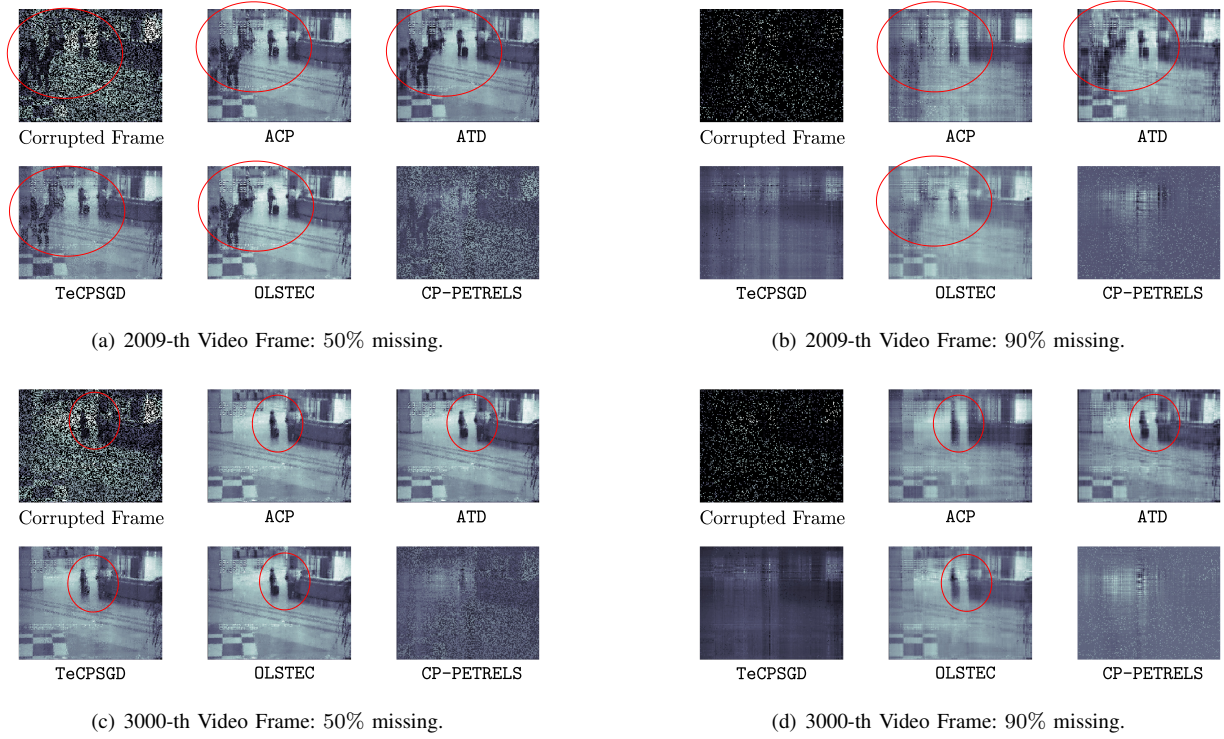


Fig. S10 – Performance of adaptive tensor decompositions on Hall data.